https://doi.org/10.5194/egusphere-2026-8
Preprint. Discussion started: 15 January 2026

Exploring the Feasibility of an Air Sensor Array for the Real-Time Detection and Characterization of VOCs

Amanda Gao[1 a], Matthew B. Goss[1 b], Erik Helstrom[1], David H. Hagan[3], Jesse H. Kroll[1,2]

[1]Department of Civil and Environmental Engineering, Massachusetts Institute of Technology, Cambridge, MA 02139, USA
[2]Department of Chemical Engineering, Massachusetts Institute of Technology, Cambridge, MA 02139, USA
[3]QuantAQ Inc., Somerville, MA 02143, USA
[a]current address: US Environmental Protection Agency, Durham, NC 27709, USA
[b]current address: Faculty of Arts and Sciences, Harvard University, Cambridge, MA 02138, USA

Correspondence to: Amanda Gao (gao.amanda@epa.gov) and Jesse Kroll (jhkroll@mit.edu)

Abstract. Volatile organic compounds (VOCs) are an important class of atmospheric chemical species that can be directly harmful to human health and contribute to the formation of hazardous secondary products. Measurements of ambient VOCs are typically made using "offline" techniques, which are well-suited for distributed measurements but have low time resolution, or real-time measurements using state-of-the-art *in situ* instruments, which have high precision and time resolution, but tend to be expensive and so cannot be deployed in a widespread manner. An alternative VOC measurement approach that is both real-time and lower in cost would open the possibility of widespread, spatially distributed measurements of VOCs in air quality and atmospheric chemistry contexts. While there are several commercially available air sensors that are sensitive to environmental VOCs, these sensors are "broadband," meaning that each can only output a single scalar value that reflects the sensitivity of the sensor toward a wide and poorly defined range of VOCs. As a result, VOC air sensors have, to date, seen little use in research. Here, we investigate the feasibility of a novel method for measuring environmental VOCs that uses an array of such broadband sensors. This array includes VOC air sensors representing three fundamentally different sensor types, and takes advantage of operational parameters that achieve a diversity of responses amongst sensors with the same type. Within a controlled laboratory setting, we obtained calibration curves for ten typical atmospheric VOCs between 5 and 100 ppb and explored the effects of varying RH and introducing binary mixtures on sensor responses. Overall, we found that all observed sensor responses can be parameterized with linear or power-law models, consistent with results of prior studies and expectations based on physical sensing principles. Our results show that each of the 12 sensors in our array appear to have their own unique sensitivities to various VOCs, resulting in distinctive "fingerprints" of array responses for each compound tested. However, we also show that interferences by water vapor and other gases pose substantial challenges that likely cannot be fully addressed in the laboratory. Thus, co-location with a reference instrument in the field may first be required if this measurement approach is to yield quantitative, chemically specific information about ambient VOCs in indoor or outdoor environments.

https://doi.org/10.5194/egusphere-2026-8
Preprint. Discussion started: 15 January 2026

1 Introduction

Measurements of atmospheric pollutants are crucial for improving our understanding of atmospheric chemistry, managing air quality, and estimating exposure to compounds that negatively affect human health. Traditionally, real-time measurements of indoor and outdoor atmospheric pollutants are made using reference instruments with high precision, sensitivity, and accuracy. However, these instruments can be prohibitively expensive in terms of cost and operating requirements. Even regions with well-developed monitoring infrastructure struggle to systematically measure the smaller, sub-regional differences in exposure (e.g., variations across cities or neighbourhoods, or even across "micro-environments" such as the home, office, or transit) that have significant effects on personal exposure and risk (Hossain et al., 2022). The high cost of these instruments also contributes to inequities in measuring air pollution: for example, air pollution disproportionately impacts low-and middle-income countries (Murray et al., 2020) yet these regions are the most likely to have an air quality data gap (Pinder et al., 2019). To fill these knowledge gaps, many researchers and regulatory bodies have begun using air sensors to make atmospheric pollutant measurements. (Here, we define "air sensors" as monitors that have a purchase cost at least one order of magnitude lower than that of a reference instrument measuring the same pollutant (Lewis et al., 2016).) Such sensors have seen major technological improvements in the last two decades, and now can measure ambient levels of atmospheric pollutants in the parts-per-billion (ppb) range (Snyder et al., 2013). In addition to their lower cost, air sensors have the added benefits of occupying little physical space, drawing low power, and generally not requiring human intervention to operate. The high spatiotemporal resolution of air sensor measurements makes them good candidates for expanding our knowledge of air quality and chemistry via novel applications such as distributed sensor networks (Mao et al., 2019), personal exposure monitors (Xie et al., 2021), and multi-pollutant sensor arrays to identify pollutant sources or transformations (Crawford et al., 2021; Hagan et al., 2019).

Air sensors have been extremely helpful in characterizing the concentrations of commonly-regulated pollutants, such as $PM_{2.5}$ (Badura et al., 2018), O_3 (Baron and Saffell, 2017), CO (Han et al., 2021), and SO_2 (Hagan et al., 2018). However, one important class of atmospheric trace species that has seen little measurement by air sensors are volatile organic compounds (VOCs). VOCs are an important class of atmospheric compounds, emitted from numerous natural sources and human activities (Guenther et al., 1995). Exposure to VOCs can be directly harmful to human health, and emitted VOCs also form hazardous secondary products, including peroxides, ozone, and secondary organic aerosol (SOA). Measurements of ambient VOCs have traditionally been made using "offline" techniques, such as sorbent tube sampling for later analysis, which are suited for distributed measurements but suffer from low time resolution (Woolfenden, 1997). For decades, real-time measurements of ambient VOCs have been made via gas-chromatography mass-spectrometry (GC-MS), but GC-MS has limited sensitivity to certain compounds and often requires pre-concentration techniques that decrease effective time resolution (Lerner et al., 2017; Pellizzari et al., 1975). The relatively recent development of novel measurement methods, such as proton-transfer reaction mass spectrometry (PTR-MS), have enabled measurements of ambient VOCs with <1 Hz time resolution. However, instruments employing these state-of-the-art measurement techniques can be extremely large, energy-consumptive, and

https://doi.org/10.5194/egusphere-2026-8
Preprint. Discussion started: 15 January 2026

expensive. Hence, a feasible sensor-based alternative would open the possibility of widespread, time-resolved, and spatially distributed measurements of VOCs in air quality and chemistry contexts.

While there are several different types of commercially available air sensors that can detect VOCs at ambient, parts-per-billion (ppb) mixing ratios, they are limited by their non-specific ("broadband") nature: individual sensors output only a single scalar value that reflects a combination of different sensor sensitivities and selectivities toward a wide and poorly-defined range of VOCs (Spinelle et al., 2017). In other words, a single sensor output can be converted to an equivalent VOC concentration by knowing a sensor's sensitivity to a particular VOC, but only if the sample air contains only that VOC. However, a single sensor's response to a VOC mixture cannot be converted to concentration units without preexisting knowledge of the mixture's composition and a detailed understanding of the sensitivity of the sensor to all VOCs in the mixture (including any gas interaction effects). As a given airmass is likely to have many VOCs with highly variable and unpredictable compositions (Chen et al., 2019), the signal from a single VOC sensor is able to provide very little useful information about total VOC concentrations, and even less about VOC composition.

A potential solution to this problem is to use multiple VOC sensors of differing selectivities. In theory, meaningful differences in responses from an array of different VOC sensors can be leveraged, via a pattern recognition algorithm, to gain useful information about the measured compound or mixture. This approach has been the linchpin of "electronic nose" studies that mostly aim to detect and classify VOC mixtures in odour detection or process control applications (Gardner and Bartlett, 1994). However, environmental VOCs pose a particular challenge for these applications: most "electronic noses" are designed to measure VOCs at high mixing ratios, generally tens or hundreds of parts-per-million (ppm), many orders of magnitude higher than the parts-per-billion (ppb) levels found in the atmosphere (Cheng et al., 2021; Gardner and Bartlett, 1994). The challenge of these measurements is further exacerbated by the complexity of atmospheric VOC sources, compositions, and variations (Luo et al., 2023; Yang et al., 2022; You et al., 2022), as well as sensor sensitivities to non-VOC gases and environmental parameters such as relative humidity and temperature (Spinelle et al., 2017).

A handful of past studies have attempted to obtain quantitative measurements of sub-ppm VOC pollution sources by utilizing arrays of metal oxide (MOx) sensors to quantify a single key VOC, and thus sidestepping the challenges posed by environmental VOC complexity. For example, methane has been an important target for several MOx sensor arrays (Domènech-Gil et al., 2024; Furuta et al., 2022; Taguem et al., 2021), which applied machine learning regression algorithms to measurements from multiple MOx sensors to estimate variations in environmental methane mixing ratios. Benzene is another important VOC that air sensors can detect sensitively, and ambient mixing ratios of benzene measured near a major roadway were accurately estimated by a neural network model trained on measurements from five different MOx sensors (De Vito et al., 2008). Similarly, Collier-Oxandale et al. (2019) used measurements from two different MOx sensors to develop regression models for atmospheric benzene, methane, and total VOC mixing ratios measured near an oil field. These studies demonstrate the potential of air sensor arrays to generate quantitative, chemically specific VOC information. However, they are somewhat limited in scope: they focus on only one or two target VOCs and use only one measurement technology (metal oxide sensing) to make measurements. Multiple other measurement technologies with sub-ppb VOC sensitivities are

https://doi.org/10.5194/egusphere-2026-8
Preprint. Discussion started: 15 January 2026

commercially available (Spinelle et al., 2017), but to our knowledge, the use of sensor arrays that use a range of sensing technologies, aimed at characterizing a wide range of VOCs, has not been explored.

Here, we investigate the feasibility of using an air sensor array for distinguishing and measuring ambient VOCs. We investigate the effectiveness of leveraging multiple different sensing technologies and examine the effects of varying operational parameters between otherwise identical sensors to obtain a larger array of distinct responses. We describe the simultaneous use of 12 distinct air sensors representing three different measurement technologies across multiple operational parameters. We also show laboratory characterization results for 10 key atmospheric VOCs (with mixing ratios from 5 to 100 ppb), as well as data from a wide range of relative humidities and a binary mixture. Finally, we discuss these results in the context of practical usage of this array for environmental monitoring, and evaluate the potential for this method to provide useful, quantitative information about VOCs in realistic ambient conditions.

2 Methods

2.1 Sensing Principles

Here, we investigate the simultaneous use of three different sensing technologies: metal oxide sensors (MOx), which measure target gas molecules that adsorb onto a metal oxide surface; photo-ionization detectors (PID), which ionize gas molecules with a small vacuum ultraviolet lamp, and amperometric electrochemical (EC) sensors, which detect gases via oxidation or reduction reactions. Each of these measurement techniques has at least one adjustable parameter that can be leveraged to obtain different VOC sensitivities between otherwise identical sensors.

Metal oxide (MOx) sensors have long been a popular choice for sensor array applications because of their particularly low material cost and relatively high sensitivity to VOCs (Cheng et al., 2021). MOx sensors measure VOCs using adsorption: gas species are chemisorbed onto the sensor surface, and the resultant band-bending by these charged molecules changes the measured conductivity (Barsan and Weimar, 2001). MOx sensors can vary in the materials or morphologies used for the semiconducting sensing layer, which can greatly affect sensing properties: past studies on MOx sensor arrays, such as those by De Vito et al. (2008) or Collier-Oxandale et al. (2019), have relied on the use of sensors with manufactured differences (e.g. distinct semiconductor properties) to introduce distinctions in sensor sensitivity that can then be exploited using pattern recognition techniques. When using an array of identical sensors rather than fundamentally different ones, it is possible to achieve differences in sensitivity and/or selectivity by varying the operation temperature (controlled by supplied voltage) of each sensor, as this affects the relationship between sensor conductance and analyte gas partial pressure (Barsan and Weimar, 2001). This technique has seen some success in electronic nose applications, such as when Liu et al. (2021) employed temperature modulation of MOx sensors to help detect excessive methanol emitted from liquors, but to our knowledge, this approach has never been applied in the context of environmental VOC measurements.

Photo-ionization detectors (PIDs), pioneered by James Lovelock to measure trace vapors in the atmosphere (Lovelock, 1960) rely on ionization of target molecules by a vacuum ultraviolet (VUV) lamp to induce a measurable change

https://doi.org/10.5194/egusphere-2026-8
Preprint. Discussion started: 15 January 2026

in electric potential that is proportional to the concentration of target gas. In theory, an array of PIDs, each containing miniature lamps of different VUV wavelengths, would be able to discriminate VOCs based on differences in ionization energy and VUV cross-sections amongst the target species. Unfortunately, PID specifications are currently limited by the state of the technology: lamps at only a small handful of wavelengths are commercially available, with 9.6 eV, 10.0 eV, and 10.6 eV being common options.

Electrochemical (EC) sensors, also known as amperometric sensors, rely on a reduction-oxidation (redox) reaction between a target gas and an aqueous acid electrolyte. Due to their high sensitivity and selectivity, they have been widely used in air quality monitoring of major inorganic pollutants such as ozone and SO_2 (Hagan et al., 2018; Lewis et al., 2016). The sensitivities of a given EC sensor to various VOCs can be adjusted via application of a bias voltage, or a potential difference between the working and reference electrodes (Baron and Saffell, 2017). EC sensors that measure VOCs non-specifically have commonly been marketed for personal protection and industrial hygiene applications; we are unaware of the use of sensitive VOC EC sensors used in atmospheric or air quality contexts.

2.2 Sensor Array Design

To investigate the utility of multiple VOC sensing technologies and operational parameters, we constructed a custom-built sensor array that includes 12 distinct VOC sensors, with a simplified schematic shown in Figure 1. The array includes three EC sensors, with one Alphasense ETO-B1 sensor and two Alphasense VOC-B1 sensors, one run without bias voltage and the other with a positive bias voltage; three PIDs, including one ION Science MiniPID 2 10.0 eV, one ION Science MiniPID 2 10.6 eV, and one ION Science iniPID High Sensitivity (HS) 10.6 eV, which achieves “high sensitivity” over the normal 10.6 PID via improvements to the sensor membrane; and six metal oxide sensors, with two different sensor models (Figaro TGS2602 and Figaro TGS2600, both SnO_2 sensors that differ in the catalyst used in their sensing materials), each run at three different supply voltages (4.75 V, 5.0 V, and 5.25 V). Table 1 summarizes the sensors used in this design and any user-controlled parameters that were applied. At the time of purchase (late 2021), the material cost of all 12 sensors was ~$2000 USD, with most of this cost made up by PIDs (with an average cost of ~$540 USD each). This total cost is higher than a typical sensor array application but is still orders of magnitudes lower than the cost of a mass spectrometric instrument.

https://doi.org/10.5194/egusphere-2026-8
Preprint. Discussion started: 15 January 2026

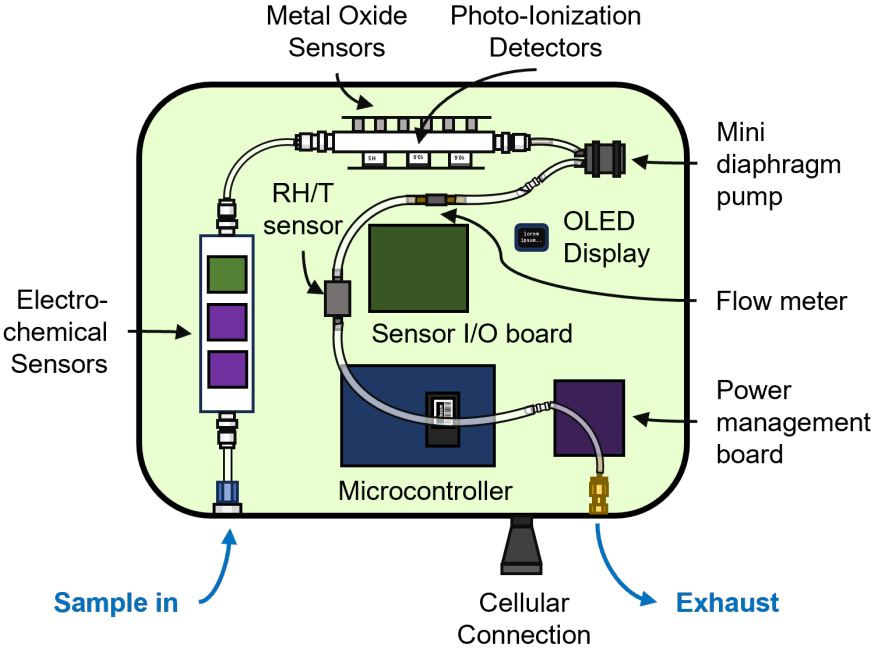

155 **Figure 1: Schematic of the VOC air sensor array. Sample air is pulled in by a miniature diaphragm pump through custom flow cells that house 12 different VOC sensors. Several custom circuit boards manage power and sensor inputs/outputs.**

Table 1: Summary of VOC air sensors used in the array.

Sensing Technology	Number of Sensors	Manufacturer	Model Name	User-Applied Parameters
EC	2	Alphasense Ltd.	VOC-B1 (EC Type 1)	Bias Voltage (1 each at 0 mV, +300 mV)
EC	1	Alphasense Ltd.	ETO-B1 (EC Type 2)	
PID	1	ION Science Ltd.	MiniPID 2 (10.0 eV)	
PID	1	ION Science Ltd.	MiniPID 2 (10.6 eV)	
PID	1	ION Science Ltd.	MiniPID HS (10.0 eV)	
MOx	3	Figaro Engineering, Inc.	TGS 2600 (MOx Type 1)	Supply voltage (1 each at 4.75 V, 5.0 V, and 5.25 V)
MOx	3	Figaro Engineering, Inc.	TGS 2602 (MOx Type 2)	Supply voltage (1 each at 4.75 V, 5.0 V, and 5.25 V)

https://doi.org/10.5194/egusphere-2026-8
Preprint. Discussion started: 15 January 2026

Air is drawn into the instrument by a miniature diaphragm pump (Xavitech v200) at a user-controlled rate that can be varied from 0-400 cm^3 min^{-1}; in this study it is set at 300 cm^3 min^{-1}. Sample air travels through PFA tubing (1/4" outer diameter, 0.190" inner diameter), into custom-made Teflon flow cells (EC flow cell has dimensions 15.0 x 3.81 x 1.90 cm, MOx/PID flow cell has dimensions of 13.5 x 3.81 x 1.90 cm), with flow perpendicular to the sensor surfaces. After the sample air is expelled from the pump, it passes through a 3D-printed enclosure containing a relative humidity (RH) and temperature (T) sensor (Sensiron SHT25) before being exhausted from the instrument. This enclosed flow-through system was chosen to enable direct introduction of known gases to the instrument (e.g. zero air for baseline measurements in the field) and better control of key environmental variables (e.g. RH), but an open system design could instead be used for passive measurements of ambient air. The design of this instrument maintains airtightness via O-rings that are flush against the sensor surfaces and mounting bolts that secure breakout circuit boards to the flow cells. Sensors are not permanently secured to either the flow cells or their respective breakout circuit boards, allowing for easy replacement of any single sensor. The fully assembled instrument is housed inside a container with dimensions 42.2 x 37.1 x 21.0 cm (PolyCase ZH-161407); this is much larger than necessary but was chosen to aid in troubleshooting this prototype instrument.

The entire device is powered by mains electricity (12 V AC/DC converter) and controlled using an LTE-enabled microcontroller (Particle B Series SoM), which is used in conjunction with its manufacturer's evaluation circuit board (Particle M2EVAL). Several custom circuit boards manage sensor input and outputs, as well as associated analog-to-digital or digital-to-analog conversion; there is also a power management circuit board that supplies lines at 3.3 V, 5.0 V, and two variable values (intended for varying MOx supply voltages) that can be adjusted from 0.64V to 5.25V via user input to a synchronous buck regulator (MIC24045). Total power draw of the instrument is highest on startup, where the microcontroller alone requires ~3 W. However, during regular operation most components have negligible power draw, but there are relatively large requirements from the pump (~0.3 W), photo-ionization sensors (~0.3 W), microcontroller (~1 W), and metal oxide sensors (~1.5 W), resulting in < 5 W of total power draw.

Data from all sensors are oversampled at ~100 Hz before being averaged down to 1 Hz. This is substantially faster than the sensor response times, but oversampling helps remove artifacts caused by electrical noise. The 1 Hz data is then logged to a local micro-SD card, and the 1-minute averages of the 1 Hz data are computed and transmitted via 3G LTE to the cloud, where they are automatically processed and stored.

2.3 Laboratory Characterization Setup

A schematic diagram of the experimental setup for characterizing sensor array responses to ppb levels of VOCs is shown in Figure 2a. To achieve low and reliable VOC mixing ratios, we use headspace sampling, in which a liquid VOC is placed in a sealed vial leaving sufficient room over the liquid, from which volatilized gas is sampled after phase equilibration. The mixing ratio of the VOC in the gas phase at equilibrium can be calculated using the compound's temperature-dependent vapor pressure. We used ten VOCs, containing several different functional groups and representing VOCs from natural and anthropogenic sources, supplied by Sigma-Aldrich: 1-hexene (purity ≥ 99.0%), 1-octene (≥ 99.5%), 2-pentanone (≥ 99.5%), 2-heptanone (≥

https://doi.org/10.5194/egusphere-2026-8
Preprint. Discussion started: 15 January 2026

99.0%), acetone (≥ 99.5%), α-pinene (≥ 98.0%), chlorobenzene (≥ 99.9%), isoprene (≥ 99.0%), *o*-xylene (≥ 99.0%), and toluene (≥ 99.8%). For each experiment, we used a gas-tight syringe to obtain a headspace VOC sample at 25 °C, then placed the syringe into a computer-controlled syringe pump (Harvard Apparatus PHD Ultra), with the syringe needle inserted into a heated inlet maintained at 50 °C to prevent condensation onto the tubing walls. A dilution stream of zero air (AADCO Model 737) was also supplied to the inlet at 10 lpm (with sample overflow managed by a tee fitting), and mass flow controllers (MKS) were used to adjust the humidity of this dilution stream by varying the ratio of dry air to air humidified by a bubbler. The syringe pump was then run with a preset, non-monotonic sequence of calibration levels, with each level being held for 25 minutes. This sequence was preceded and followed by 30 minutes of zero air for baseline correction. Finally, after the calibration sequence was completed, the syringe was flushed with zero air several times before the next injection. An example calibration sequence, with sample sensor responses, is shown in Figure 2b.

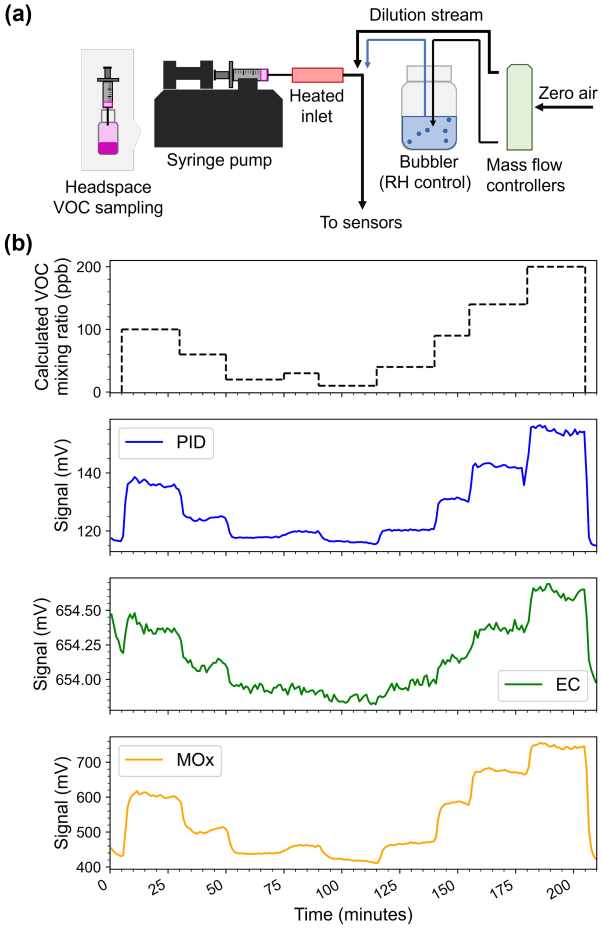

Figure 2: (a) Schematic of the experimental apparatus. The VOC calibration gas system consists of gas-phase VOC obtained via headspace sampling that is then loaded into a gas-tight syringe and injected using a computer-controlled syringe pump. This is then diluted by a stream of zero air that can be humidified by a bubbler. The total flow is 10 lpm, with sample air vented before reaching the instruments. (b) Example calibration sequence for a sample VOC (isoprene at 35% RH), with compound concentration shown in the top panel by the dotted black line. Sample responses from one PID (HS PID), EC (EC Type 1, no bias), and MOx (MOx Type

https://doi.org/10.5194/egusphere-2026-8
Preprint. Discussion started: 15 January 2026

1, 5.0 V) sensor from the array are shown in the lower panels. Note that y-axes do not start at 0, and that this sequence spans 0 to 200 ppb for demonstrative purposes.

From each calibration sequence, we average the steady-state values of sensor responses and derive a calibration curve, or sensor signal as a function of mixing ratio. Sensor responses do not respond immediately to changes in mixing ratio, and calculated time constants fell within a wide range of values (0.5-10 min^{-1}) and appear to depend on the specific compound, sensor, and magnitude of the mixing ratio step change. A detailed characterization of these time constants is beyond the scope of this study. Instead, we ignore the transient nature of these sensor responses by holding each mixing ratio level for at least 20 minutes and generating points in the calibration curve by averaging the last 5 minutes of sensor responses for each mixing ratio. Sensor responses are described in terms of net change in signal (increase over baseline). We `prioritize characterization of signal changes (sensitivities) over characterization of baseline values, as we expect that most practical applications of these sensors will involve baseline removal prior to data analysis. Characterization of baseline changes and drift, which are expected to vary with the humidity and composition of background air (Wang et al., 2010; Wei et al., 2018), is beyond the scope of this work but would be a useful target for future research. In our dataset, most baseline values were removed by a simple background subtraction. Some experiments showed mild drift between beginning and end values (<2% of the difference between signal at 100 ppb and beginning background signal), usually caused by changes to relative humidity over the course of the experiment. In these situations, the PID and EC baseline for PIDs and ECs was identified and removed using the BaselineRemoval Python library (v1.0.5). The results from two different modified second-degree polynomial fits (ModPoly (Lieber and Mahadevan-Jansen, 2003) and IModPoly (Zhao et al., 2015)) were calculated, and the best of these methods was identified by minimizing calibration curve fit error.

3 Results

3.1 Sensor Array Responses to Individual VOCs

Sensor responses to 10 VOCs, broadly representative of those found in the atmosphere, were obtained in the range of 5 to 100 ppb at a constant relative humidity of 30% and a temperature of 22 °C. The sensor responses to these compounds (1-hexene, 1-octene, 2-pentanone, 2-heptanone, acetone, α-pinene, chlorobenzene, isoprene, *o*-xylene, and toluene) are summarized in Figure 3 and Table S1 in the Supporting Information. In many cases a given sensor exhibits low (even negligible) sensitivity to a given VOC; in the discussion below, we consider a sensor to "detect" a compound if a calibration curve can be fit to a nonzero sensitivity with at least 1σ confidence.

All photo-ionization detectors (PIDs) consistently exhibited a linear signal-to-mixing ratio response across this range of mixing ratios, and this linearity is consistent with the results of prior studies on these sensors (Freedman, 1980; Lovelock, 1960). The "high-sensitivity" (HS) PID (10.6 eV) was able to detect all 10 compounds, with sensitivities ranging from 5.0×10^{-2} ($\pm$ 1.5×10^{-3}) mV/ppb for *o*-xylene to 1.8 ($\pm$ 4.6×10^{-2}) mV/ppb for acetone. (All reported confidence intervals are ±1σ.)

https://doi.org/10.5194/egusphere-2026-8
Preprint. Discussion started: 15 January 2026

Sensitivities for the other two PIDs (ION science MiniPID 10.0 and 10.6 eV sensors) were substantially lower, with a range of 6.0×10^{-4} ($\pm 3.0\times10^{-4}$) to 3.3×10^{-2} ($\pm 7.2\times10^{-3}$) mV/ppb for the 10.0 eV PID, and 1.7×10^{-3} ($\pm 3.0\times10^{-4}$) to 8.1×10^{-2} ($\pm 2.0\times10^{-3}$) mV/ppb for the 10.6 eV PID. Unlike the high-sensitivity PID, neither sensor detected the full set of compounds.

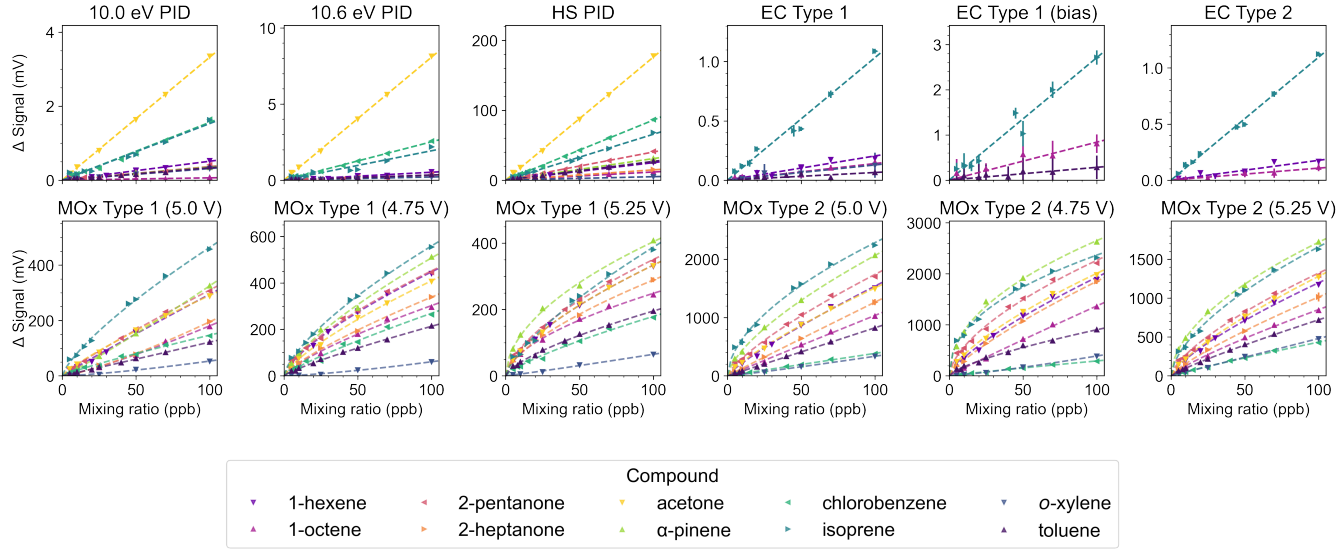

Figure 3: Summary of sensor responses (in mV over baseline) to various VOC mixing ratios between 5-100 ppb at 30% RH. Dotted lines represent the linear least-squares regression (PID and EC) or the power-law fit (MOx) of the measured values, denoted by triangles. Note that y-axes are not shared across panels, reflecting the wide range of sensitivities across sensors. If a compound is missing from a sensor's subplot, as is the case with EC sensors (second row), it means that the sensor does not exhibit sensitivity to that compound above its baseline noise. Error bars denote the standard deviation of measurements taken for each data point.

Signals from the EC sensors were also linear with mixing ratio, as reported previously (Mead et al., 2013). However, in contrast to PIDs, they detected only a subset of compounds and exhibited lower sensitivities. EC Type 1 (Alphasense VOC-B1 EC sensor) detected five compounds, with sensitivities ranging from 6.6×10^{-4} ($\pm 3.6\times10^{-4}$) mV/ppb (toluene) to 1.0×10^{-2} ($\pm 1.2\times10^{-3}$) mV/ppb (isoprene). Application of a positive bias voltage generally increased sensor sensitivity to detected compounds: for example, the sensitivity of the biased sensor to isoprene was determined to be 2.7×10^{-2} ($\pm 8.0\times10^{-3}$) mV/ppb, nearly triple the value of the unbiased sensor. However, the biased sensor exhibited substantial baseline drift, leading to larger uncertainties in sensitivities and potentially masking the sensor response to some compounds (1-hexene and *o*-xylene) that the unbiased sensor was able to detect reliably. The second EC type in our array (Alphasense ETO-B1), measured three compounds with sensitivities ranging from 1.1×10^{-3} ($\pm 2.2\times10^{-4}$) mV/ppb (1-octene) to 1.1×10^{-2} ($\pm 6.4\times10^{-4}$) mV/ppb (isoprene). The VOC sensitivities of these Type 2 sensors are very close in absolute value to the sensitivities of the unbiased Type 1 sensor, but the Type 2 sensor detects fewer compounds than the unbiased Type 1 sensor does.

Each metal oxide (MOx) sensor detected all ten compounds, but with distinctly nonlinear calibration curves. A power-law relationship describes the observed signals well, and is consistent with MOx physical sensing principles which predict a power law relationship based on the kinetics of MOx surface reactions and a balance on the availability of surface sites (Barsan

https://doi.org/10.5194/egusphere-2026-8
Preprint. Discussion started: 15 January 2026

and Weimar, 2001). The observed responses, in terms of change in voltage over baseline, can be expressed as $\Delta V = A[VOC]^{\beta}$, where A is a measure of sensitivity (in mV $ppb^{-\beta}$) and β is a dimensionless power-law parameter. Averaged MOx calibration points were fit to this expression using a nonlinear least-squares regression. Many MOx sensor studies report signal in terms of a resistance ratio R/R_0, where R is the sensor resistance to a target gas and R_0 is the baseline resistance of the sensor in clean air; we choose to report output voltage to stay consistent with the other sensors in the array. The relationship between output voltage and the resistance ratio can be generally described with $R/R_0 \propto V_c/V_{out} - 1$, where V_{out} is the output voltage and V_c is the measurement circuit voltage (equal to 5 V for all our sensors).

The two models of metal oxide sensors have very different sensitivity ranges to the VOCs tested: MOx Type 1 (TGS2600) responses was most sensitive to isoprene, with a sensitivity of 22 (± 5.1) mV $ppb^{-\beta}$ (with $\beta = 0.70 \pm 0.040$), while MOx Type 2 (TGS2602) was most sensitive to α-pinene, with a sensitivity of 140 (± 29) mV $ppb^{-\beta}$ ($\beta = 0.67 \pm 0.040$). Further differences in sensitivity were achieved by varying the circuit voltage applied to individual sensors, which changes the operating temperature of each sensor. We observe that both the sensitivity A and the power law parameter β vary among sensors, but we are unable to generalize the relationship between these parameters and applied voltage across all compounds. This finding is consistent with the results of Wang et al. (Wang et al., 2010), who observed that the dependence of MOx VOC sensitivities on operating temperature is non-monotonic and compound-specific.

Figure 4 summarizes the responses of the array to all ten compounds at 10 ppb, with signals normalized to each sensor's maximum observed response (ΔV) across all VOCs tested (note that the relative scaling of sensor responses is impacted by the high measurement error from the biased EC Type 1 sensor). In general, we observe that all ten compounds are detected by sensors that represent at least two distinct sensor types. Across compound types, there are some clear differences in overall array sensitivity: for example, alkenes are well-detected, while aromatics are not. Moreover, each compound has a unique "fingerprint" of relative sensor responses, even when compounds are chemically similar: for example, the array's response to 1-hexene can clearly be distinguished from the response to 1-octene. Fig. 4 indicates that different sensing technologies, as well as variations within the same sensing technology, exhibit different responses to VOCs, with each of the 12 sensors exhibiting their own unique sensitivities to various VOCs. From this dataset, we are unable to identify broad patterns in sensor array response for different VOCs, due in part to the relatively limited set of VOCs tested. Nonetheless, Figure 3 shows that an array of "broadband" sensor responses can indeed be used to distinguish different VOCs.

https://doi.org/10.5194/egusphere-2026-8
Preprint. Discussion started: 15 January 2026

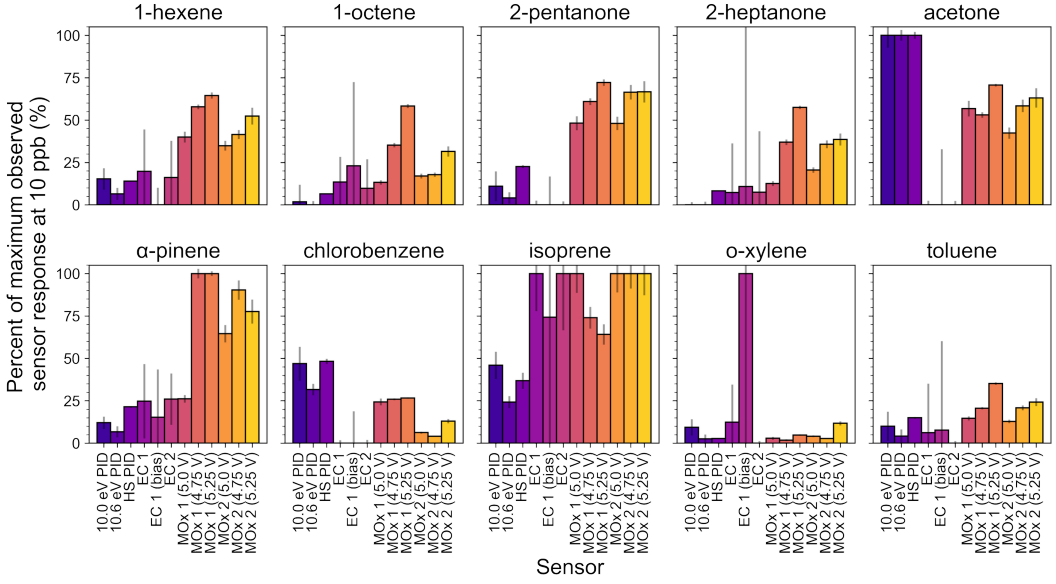

Figure 4: Summary of sensor responses to 10 different VOCs at 10 ppb. Sensitivities are given as a percentage of the maximum observed response for each individual sensor across all VOCs tested. Error bars are calculated using propagation of the 1σ measurement errors shown in Figure 3: if a sensor has a response of x + Δx mV to a certain compound, and has a maximum response of y + Δy mV, then the error Δz of the fractional response z = x/y is calculated from $\Delta z = z[(\Delta x/x)^2 + (\Delta y/y)^2]^{1/2}$.

3.2 Sensor Array Responses as a Function of Relative Humidity

Environmental parameters (temperature and relative humidity) are known to impact air sensor VOC measurements. Characterizing sensor responses to changing environmental temperature is beyond the scope of this study, as ambient temperature does not have a large effect on EC sensor or PID responses (Adamia et al., 1991; Hitchman and Saffell, 2021), though it could impact the baseline responses of MOx sensors (Figaro USA Inc., 2013; Figaro USA Inc., 2015; Wang et al., 2010). To explore the effects of relative humidity (RH) on sensor responses, we obtained calibration curves between 5 and 100 ppb for two VOCs (α-pinene and isoprene) across a wide range of RH values (0%-90%). Results are shown in Figures 5 and 6.

https://doi.org/10.5194/egusphere-2026-8
Preprint. Discussion started: 15 January 2026

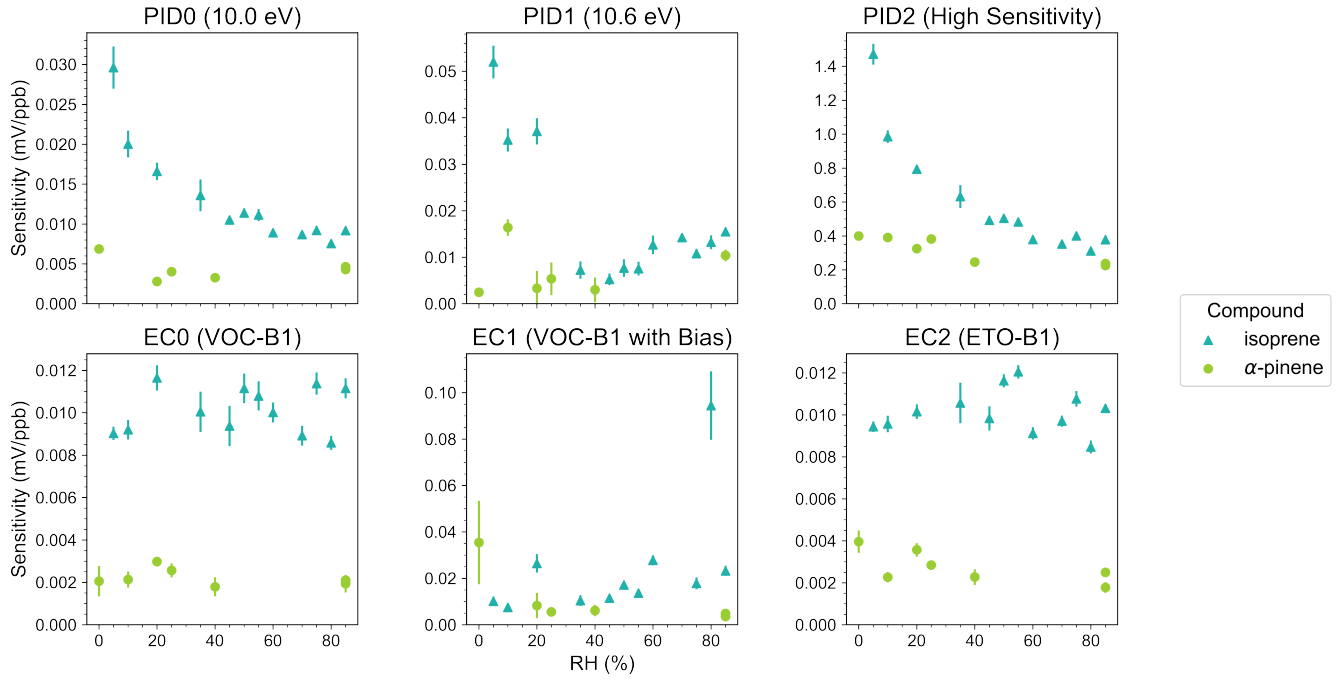

Figure 5: Sensitivities (in mV/ppb) of 3 PIDs (top row) and (b) 3 EC sensors (bottom row) to isoprene and α-pinene as a function of RH. Vertical bars denote 1σ confidence intervals. Note that each panel features different y-axes.

Figure 5 shows the effect of RH on sensitivity for PID and EC sensors, both of which have linear calibration curves. The top row demonstrates the dramatic effect water vapor can have on PID responses. This decrease in sensor signal is likely explained by the absorption of UV radiation by water vapor, which reduces ionization efficiency (Liess and Leonhardt, 2003). While it has been reported that RH can also increase PID responses via water contamination of the sensor's electrodes, leading to an artificially high signal output due to short-circuiting (Scott, 2020), our results suggest that the PIDs in our array do not experience this effect. Instead, sensor responses generally decrease in a monotonic and nonlinear fashion with increasing RH. Moreover, the RH-induced decrease in sensitivity is larger for isoprene than it is for α-pinene, indicating that this effect is compound-specific. Unfortunately, the nonlinear and compound-specific relationship between PID sensitivity and RH does not seem to be easily parameterizable. Ultimately, while our PIDs may involve technologies that aim to prevent sensitivity decreases under high humidity conditions, these results suggest that PID responses can still be strongly and unpredictably dependent on RH.

The bottom row of Figure 5 shows EC sensitivity to isoprene and α-pinene as a function of RH. Unlike the PID sensors, EC sensors do not show clear trends with increasing RH for either compound. This is in contrast to previous work, which found that exposure to water vapor can affect responses because of RH-induced changes in the sensor electrolyte that affect the kinetics and thermodynamics of electro-oxidation (Farquhar et al., 2021). Water vapor has also been found to affect long-term EC responses (Hitchman and Saffell, 2021), but this is beyond the scope of this study. EC signals were generally

https://doi.org/10.5194/egusphere-2026-8
Preprint. Discussion started: 15 January 2026

much noisier than other sensors, and thus any trends in sensitivity might be partially obscured by this high noise level. However, these results suggest that, without considering long-term effects, RH does not have a clear impact on EC sensitivity to these VOCs.

The effects of RH on MOx sensor responses are more complicated, due to changes in both the power law response parameters. Figure 6 shows responses of one Type 1 and one Type 2 MOx (both operated at 5.25V) to isoprene and α-pinene at different RH values, in terms of the response parameters A and β (the associated calibration curves are shown in Figure S1 in the Supporting Information). For MOx sensors, an increase in humidity can cause decreased resistance and an increase in electron affinity, which induces compound-specific changes in response (Fine et al., 2010). This effect is dependent on the sensor's operating temperature, and should be less pronounced at higher temperatures (Bârsan and Weimar, 2003; Korotcenkov et al., 2007). We were particularly interested to see if changes in MOx response caused by RH changes could be parameterized in terms of the sensitivity A and the power-law coefficient β, as prior work suggests that SnO_2 sensors measuring certain organic compounds obey a simple relationship (log(A) ~ β) under changing humidity (Chabanis et al., 2003). For MOx type 2 (right panel of Figure 6), this relationship holds across relative humidity and compounds; moreover, in most cases an increase in RH causes an increase in the power law coefficient and a logarithmic decrease in the sensitivity. This suggests that, with more data, it may be possible to accurately predict the effect of changing RH on MOx Type 2 responses to VOCs; though this is expected to be heavily compound-specific, as certain VOCs do not exhibit this response behaviour (Chabanis et al., 2003). However, the relationship between fit parameters is markedly less clear for MOx type 1 (left panel of Fig. 5), as there does not appear to be a consistent relationship between increasing RH and β.

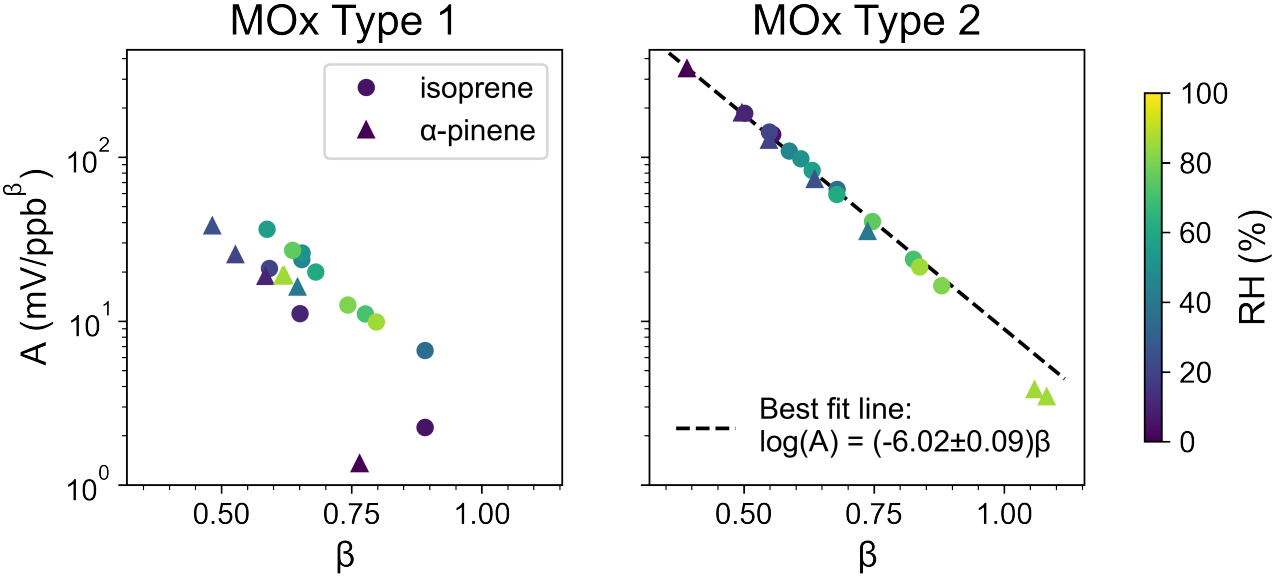

Figure 6: MOx responses to isoprene (circles) and α-pinene (triangles), plotted in the parameter space of the power-law parameter β (dimensionless) vs. sensitivity A (mV/ppb^{β}). The dotted black line gives the best fit line for all data measured for MOx Type 2.

https://doi.org/10.5194/egusphere-2026-8
Preprint. Discussion started: 15 January 2026

3.3 Sensor Array Responses to Binary Mixtures

Real-world environmental VOCs are almost always present within complex mixtures, which poses a measurement problem for non-specific VOC sensors such as the ones examined here. Additivity of air sensor responses to mixture components would help to simplify this problem, but because of the potential for cross-interferences between VOCs such additivity is not a given. To investigate this, we exposed the sensor array to two binary mixtures of 1-hexene and 1-octene, with molar ratios of 1:1 and 3:1.

Figure 7 shows binary mixture responses of PID and EC sensors to the two binary mixtures; for simplicity, results for only the most sensitive sensors are shown. Table S2 in the Supporting Information summarizes the fitted sensitivities to each mixture. For the high-sensitivity PID, the mixture measurement is consistent with linear additivity: sensitivity is 2.5×10^{-1} ($\pm$ 4.2×10^{-3}) mV/ppb to 1-hexene and 1.2×10^{-1} ($\pm$ 2.1×10^{-3}) mV/ppb to 1-octene, and the observed sensitivity to the 1:1 mixture is $1.7 \times 10^{-1} \pm (2.3 \times 10^{-3})$ mV/ppb (expected 1.8×10^{-1} mV/ppb), while the observed sensitivity to the 3:1 mixture is 2.0×10^{-1} ($\pm$ 3.4×10^{-3}) mV/ppb (expected 2.1×10^{-1} mV/ppb). The 10.0 eV also showed a proportional response to the 1:1 mixture, and the observed 3:1 sensitivity falls close to the expected value. The EC sensor signals (bottom panels of Figure 7) also obey additivity within uncertainty, though the high measurement noise makes the EC mixture response uncertainties much higher than those of PIDs. The observed linearly additive nature of these sensor responses to mixtures is consistent with expectations based on the principles of operation of PID and EC sensors (Baron and Saffell, 2017; Freedman, 1980).

https://doi.org/10.5194/egusphere-2026-8
Preprint. Discussion started: 15 January 2026

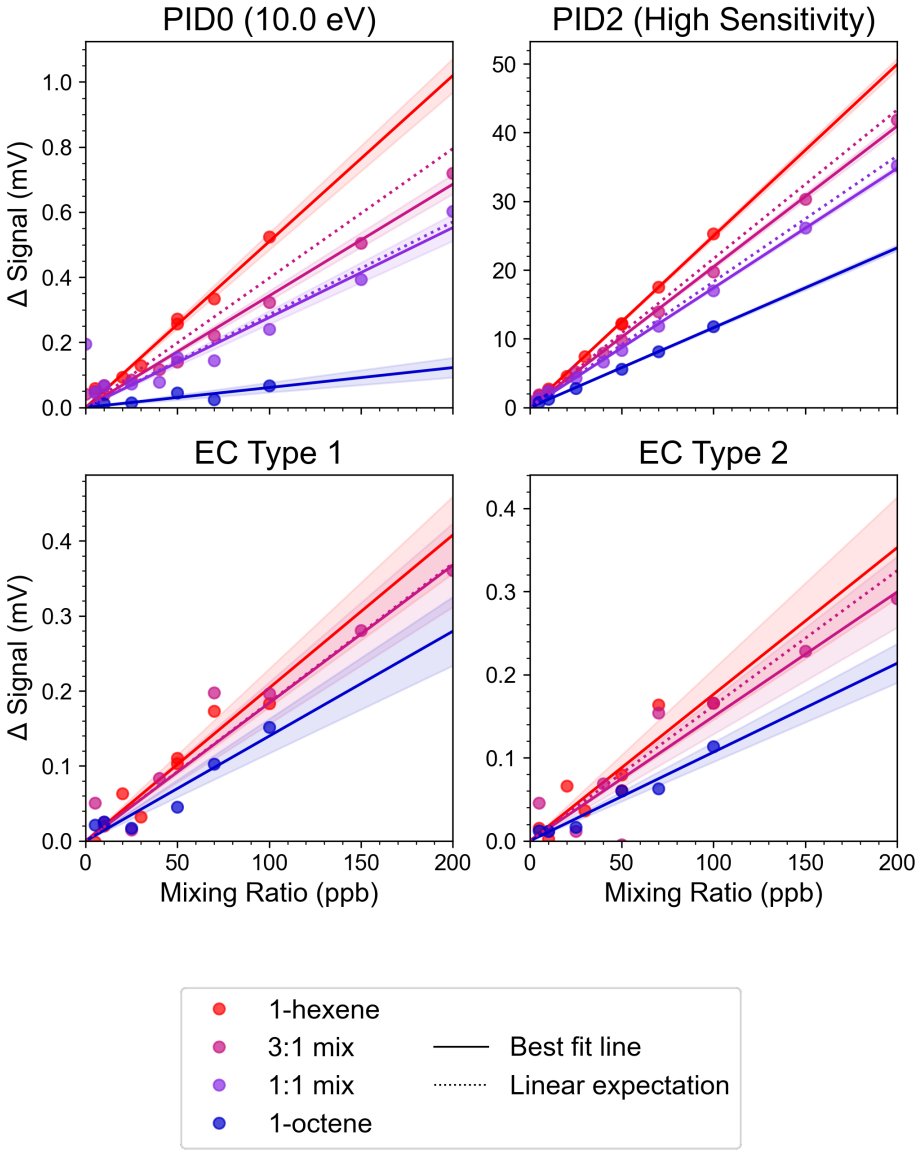

Figure 7: Sensor responses to 1:1 (purple) and 3:1 (magenta) mixtures of 1-hexene (red) and 1-octene (blue), for (a) two PIDs and (b) two EC sensors. Solid lines indicate the best fit line for each of the points, and the shaded area indicates the 1σ confidence interval; dotted lines indicate the expected signal assuming additivity. The mixing ratio (x axis) refers to the total amount of VOC (i.e., both components of the mixtures) introduced to the sensors. Note that for EC Type 1, the dashed 3:1 mix line partially obscures the respective dotted line. EC measurements of the 1:1 mixture are missing due to issues with the EC power supply.

The response of MOx sensors to binary mixtures is more complex. Figure 8 shows the response of two MOx sensors to the same binary mixtures (1:1 and 3:1 molar ratios of 1-hexene and 1-octene), as well as the expected results of linearly combining the power law response curves. For both sensors, the observed mixture response is far below this predicted sum, at least at higher mixing ratios (>10 ppb). This indicates that different VOCs can interact with each other on the MOx sensor,

https://doi.org/10.5194/egusphere-2026-8
Preprint. Discussion started: 15 January 2026

leading to a response that is not a linear combination of the individual power law response curves. This is consistent with the work of Llobet et al. (1998), who showed that linear addition was an acceptable approximation at low mixing ratios, but found that MOx responses at higher mixing ratios required the inclusion of an interaction term for each gas pair from the total sum of responses. Llobet et al. found that the response of a MOx sensor to a binary mix of VOC_1 and VOC_2 could be represented as $A_1[VOC_1]^{\beta 1} + A_2[VOC_2]^{\beta 2} - A_{12}[VOC_1]^{\beta 1}[VOC_2]^{\beta 2}$ (Llobet et al., 1998). We applied this equation to our own mixture data, calculating a coefficient A_{12} that represents the interaction between 1-hexene and 1-octene. Calculated values of A_{12} were found to be consistent across the different mixture proportions: for the MOx type 1 sensor, we found $A_{12} = 2.9 \times 10^{-3}$ ($\pm 1.3 \times 10^{-4}$) and $A_{12} = 3.4 \times 10^{-3}$ ($\pm 2.0 \times 10^{-4}$) for the 1:1 and 3:1 mixtures, respectively; for the MOx type 2 sensor, $A_{12} = 5.3 \times 10^{-4}$ ($\pm 1.3 \times 10^{-4}$) and $A_{12} = 5.7 \times 10^{-4}$ ($\pm 2.0 \times 10^{-4}$) for the 1:1 and 3:1 mixtures, respectively. Our results suggest that while the MOx signals may be additive at low levels of VOC (10 ppb or lower), the additivity approximation is inaccurate at higher levels, and that the inclusion of VOC-VOC interaction terms (Llobet et al., 1998) is necessary for accurate estimates of VOC levels.

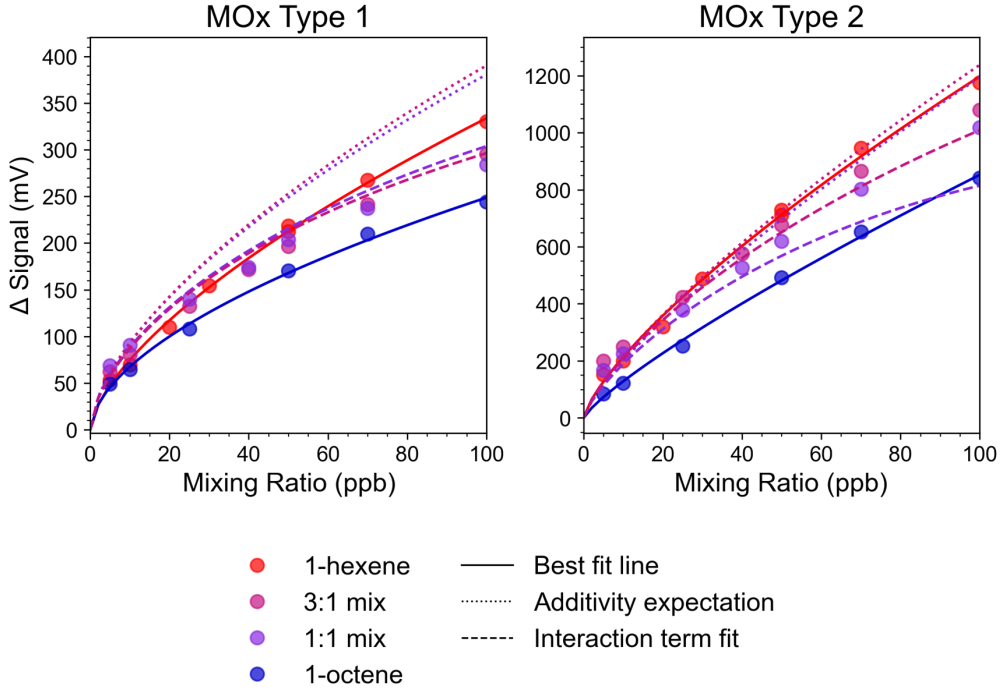

Figure 8: MOx responses to 1:1 (purple) and 3:1 (magenta) mixtures of 1-hexene (red) and 1-octene (blue). Solid lines: best fit of each VOC or mixture; dotted lines: the predicted mixture signal, assuming additivity; dashed lines: predicted mixture signal that includes a fitted interaction term (Llobet et al., 1998). The mixing ratio (x axis) refers to the total amount of VOC (i.e., both components of the mixtures) introduced to the sensors.

https://doi.org/10.5194/egusphere-2026-8
Preprint. Discussion started: 15 January 2026

4 Discussion

Figure 4 highlights the potential of the sensor-array approach for characterizing VOCs: for ten different VOCs at relatively low (10 ppb) mixing ratios, the responses from an array of broadband sensors provides unique information about the given VOC. However, our work on RH effects and mixture responses highlights major challenges for transferring laboratory results to the practical application of this approach, as both effects are substantial and difficult to parameterize. In a real atmospheric environment where such a sensor array might be used, RH will likely fluctuate, and the VOCs being sampled will almost certainly be present in complex mixtures. Thus, it is important to understand the limitations of this sensor-array measurement approach, and possible ways to mitigate the challenges posed by mixtures and RH.

One potential solution to the RH and mixture problems is to carry out a complete, prescriptive laboratory study that exhaustively determines sensor sensitivity responses as a function of RH and the VOC in question, as well as MOx interaction terms for many different gas pairings. However, such a characterization is not easily scalable: the real atmosphere contains far too many VOCs, with too many RH conditions and possible VOC mixture compositions, for such prescriptive lab characterization to be feasible. Consider the hypothetical case of fully characterizing sensor responses to 30 important environmental VOCs (a conservative number given the complexity of ambient air). Sensor characterization at three concentrations and three RH values (low, medium, high) would require a minimum of 270 individual measurements, and if binary MOx interaction terms were desired the number of experiments would drastically increase due to the 435 possible unique pairings. This assumes that the MOx interaction terms are binary only; if sensitivity is also affected by interactions among three or more VOCs, this number of experiments becomes much larger still.

Alternatively, it is possible to limit the effects of RH on sensor measurements by choosing practical applications without large RH variance. Our laboratory results suggest that RH extremes pose the largest challenge to the sensor array. At low values of RH (between 0 and 30%), the effect of RH on PID and MOx sensitivities is large and highly nonlinear, and EC sensors will also experience gradual dehydration (Hitchman and Saffell, 2021). At high RH, sensor sensitivity becomes far less dependent on RH, though degradation of PID and MOx sensors could occur after prolonged exposure. To avoid these RH-related issues, an ideal use case for this instrument would involve measurements of air either maintained at a constant and moderate RH level, or limited to a narrow range of moderate RH values (e.g. 40-60% RH). For example, a sensor array could be used to make measurements of VOCs in indoor environments, which are generally maintained at this moderate RH range. If measurements of outdoor VOCs are desired, the sensor array could potentially be placed downstream of humidity-removal techniques that remove water while preserving water-soluble sample VOCs (Beghi and Guillot, 2006; Lee et al., 2019, 2023),

The problem posed by VOC mixtures could potentially be addressed by carrying out calibrations that are specifically tailored to environmental applications: for example, calibrations could focus on characterizing the array's responses to mixtures that are representative of realistic atmospheric VOC sources, such as biomass burning and traffic. Calibration could also be carried out via sensor co-location with reference instruments, a technique that has been used in air sensor studies to effectively calibrate key pollutants such as SO_2 (Hagan et al., 2018), NO_2 (Zamora et al., 2023), and PM (Zusman et al., 2020).

https://doi.org/10.5194/egusphere-2026-8
Preprint. Discussion started: 15 January 2026

Co-location has many advantages: the reference instruments are sensitive, specific, reliable, and regularly calibrated. Such a calibration for VOC measurements would be challenging, but is possible through the co-location of sensors with a research-grade instrument that measures multiple VOCs (e.g., GC-MS or PTR-MS), and the novel application of data analysis techniques that directly interpret air sensor measurements made in the field.

5 Conclusion

We investigated the feasibility of using an array of air sensors to make measurements of VOCs. This array consists of 12 total PID, MOx, and EC sensors, each with their own unique sensitivities to VOCs. We investigated the array's responses to 10 representative VOCs between 5-100 ppb in a controlled laboratory environment, and results highlight the potential of such a sensor array in making measurements of VOCs: the entire array of responses clearly gives us unique information about the VOC being measured (Figure 4). We also explored the effects of changing RH: PIDs showed a consistent but VOC-specific decrease in sensitivity with increasing RH, EC sensor sensitivities changed only slightly or in a predictable manner, and one type of MOx sensor saw changes in its signal fit parameters that were consistent across different RH values, but the other MOx type saw substantial and unpredictable changes in signal due to RH. For a simple binary mixture, we found that PIDs and EC signals showed additivity, while MOx sensors did not. All obtained results are consistent with our expectations based on prior studies and physical sensing principles. RH and mixture effects on sensor responses do pose some problems for practical usage of this measurement approach, but these effects can likely be mitigated by limiting RH variability or employing alternative calibration techniques, such as co-location with a reference instrument.

Our results have focused on key aspects of the sensor array's responses, but there are other attributes of sensor responses that should be characterized in the future. We did not investigate the transient behaviour of these sensors (e.g., signal response and decay times) in detail, nor did we quantify baseline drift caused by ambient temperature changes or sensor aging. These aspects of sensor responses are important areas for future work to address. In addition, this study focuses on a single combination of commercially available sensors and operational parameters, but as new VOC air sensors become available, these too could be incorporated into future studies, potentially leading to an even larger matrix of distinct responses.

In summary, our laboratory results demonstrate a proof-of-principle for future applications of VOC air sensor arrays. Although environmental applications pose unique challenges that cannot all be prescriptively addressed in the laboratory, we show that this approach has promise for yielding quantitative, chemically specific information about VOCs. Ultimately such an approach could enable lower-cost, distributed VOC measurements, which in turn will contribute to our fundamental understanding of atmospheric chemical composition and human exposure to air pollutants across a wide range of scales.

Author Contributions

https://doi.org/10.5194/egusphere-2026-8
Preprint. Discussion started: 15 January 2026

AG: conceptualization, formal analysis, methodology, software, validation, visualization, writing – original draft and writing – review and editing. MBG: methodology, writing – review and editing. EH: methodology. DHH: conceptualization, methodology. JHK: conceptualization, supervision, and writing – review and editing.

Competing interests

The authors declare that they have no conflict of interest.

Acknowledgements

This work was supported by the Alfred P. Sloan Foundation's "Chemistry of Indoor Environments" program under grant number G-2018-11096 and the United States Environmental Protection Agency (assistance agreement RD-84042501). This work is not a product of the United States Government or the United States Environmental Protection Agency, and the author is not doing this work in any governmental capacity. The contents of this document do not necessarily reflect the views and policies of the Environmental Protection Agency, nor does the EPA endorse trade names or recommend the use of commercial products mentioned in this document.

Data Availability

All figure data are available via the Kroll Group publication website at http://krollgroup.mit.edu/publications.html (Kroll Group, 2025).

References

Adamia, T. V., Budovich, V. L., Nevjagskaya, I. A., Shlyakhov, A. F., and Jakovlev, S. A.: Effect of temperature on the sensitivity of the photoionization detector, Journal of Chromatography A, 540, 441–448, https://doi.org/10.1016/S0021-9673(01)88836-1, 1991.

Figaro USA, Inc: TGS 2600 Product Information, 2013. https://www.figarosensor.com/product/docs/TGS2600B00%20%280913%29.pdf, last access: 31 December 2025.

Figaro USA, Inc: TGS 2602 Product Information, 2015. https://www.figarosensor.com/product/docs/TGS2602-B00%20%280615%29.pdf, last access: 31 December 2025.

Badura, M., Batog, P., Drzeniecka-Osiadacz, A., and Modzel, P.: Evaluation of Low-Cost Sensors for Ambient $PM_{2.5}$ Monitoring, Journal of Sensors, 2018, e5096540, https://doi.org/10.1155/2018/5096540, 2018.

Baron, R. and Saffell, J.: Amperometric Gas Sensors as a Low Cost Emerging Technology Platform for Air Quality Monitoring Applications: A Review, ACS Sens., 2, 1553–1566, https://doi.org/10.1021/acssensors.7b00620, 2017.

https://doi.org/10.5194/egusphere-2026-8
Preprint. Discussion started: 15 January 2026

Barsan, N. and Weimar, U.: Conduction Model of Metal Oxide Gas Sensors, Journal of Electroceramics, 7, 143–167, https://doi.org/10.1023/A:1014405811371, 2001.

Bârsan, N. and Weimar, U.: Understanding the fundamental principles of metal oxide based gas sensors; the example of CO sensing with SnO_2 sensors in the presence of humidity, J. Phys.: Condens. Matter, 15, R813, https://doi.org/10.1088/0953-8984/15/20/201, 2003.

Beghi, S. and Guillot, J.-M.: Sample water removal method in volatile organic compound analysis based on diffusion through poly(vinyl fluoride) film, Journal of Chromatography A, 1127, 1–5, https://doi.org/10.1016/j.chroma.2006.05.102, 2006.

Chabanis, G., Parkin, I. P., and Williams, D. E.: A simple equivalent circuit model to represent microstructure effects on the response of semiconducting oxide-based gas sensors, Meas. Sci. Technol., 14, 76–86, https://doi.org/10.1088/0957-0233/14/1/312, 2003.

Chen, X., Millet, D. B., Singh, H. B., Wisthaler, A., Apel, E. C., Atlas, E. L., Blake, D. R., Bourgeois, I., Brown, S. S., Crounse, J. D., de Gouw, J. A., Flocke, F. M., Fried, A., Heikes, B. G., Hornbrook, R. S., Mikoviny, T., Min, K.-E., Müller, M., Neuman, J. A., O'Sullivan, D. W., Peischl, J., Pfister, G. G., Richter, D., Roberts, J. M., Ryerson, T. B., Shertz, S. R., Thompson, C. R., Treadaway, V., Veres, P. R., Walega, J., Warneke, C., Washenfelder, R. A., Weibring, P., and Yuan, B.: On the sources and sinks of atmospheric VOCs: an integrated analysis of recent aircraft campaigns over North America, Atmospheric Chemistry and Physics, 19, 9097–9123, https://doi.org/10.5194/acp-19-9097-2019, 2019.

Cheng, L., Meng, Q.-H., Lilienthal, A. J., and Qi, P.-F.: Development of compact electronic noses: a review, Meas. Sci. Technol., 32, 062002, https://doi.org/10.1088/1361-6501/abef3b, 2021.

Collier-Oxandale, A. M., Thorson, J., Halliday, H., Milford, J., and Hannigan, M.: Understanding the ability of low-cost MOx sensors to quantify ambient VOCs, Atmospheric Measurement Techniques, 12, 1441–1460, https://doi.org/10.5194/amt-12-1441-2019, 2019.

Crawford, B., Hagan, D. H., Grossman, I., Cole, E., Holland, L., Heald, C. L., and Kroll, J. H.: Mapping pollution exposure and chemistry during an extreme air quality event (the 2018 Kīlauea eruption) using a low-cost sensor network, Proceedings of the National Academy of Sciences, 118, e2025540118, https://doi.org/10.1073/pnas.2025540118, 2021.

De Vito, S., Massera, E., Piga, M., Martinotto, L., and Di Francia, G.: On field calibration of an electronic nose for benzene estimation in an urban pollution monitoring scenario, Sensors and Actuators B: Chemical, 129, 750–757, https://doi.org/10.1016/j.snb.2007.09.060, 2008.

Domènech-Gil, G., Duc, N. T., Wikner, J. J., Eriksson, J., Påledal, S. N., Puglisi, D., and Bastviken, D.: Electronic Nose for Improved Environmental Methane Monitoring, Environ. Sci. Technol., 58, 352–361, https://doi.org/10.1021/acs.est.3c06945, 2024.

Farquhar, A. K., Henshaw, G. S., and Williams, D. E.: Understanding and Correcting Unwanted Influences on the Signal from Electrochemical Gas Sensors, ACS Sens., 6, 1295–1304, https://doi.org/10.1021/acssensors.0c02589, 2021.

Fine, G. F., Cavanagh, L. M., Afonja, A., and Binions, R.: Metal Oxide Semi-Conductor Gas Sensors in Environmental Monitoring, Sensors, 10, 5469–5502, https://doi.org/10.3390/s100605469, 2010.

Freedman, A. N.: The photoionization detector: Theory, performance and application as a low-level monitor of oil vapour, Journal of Chromatography A, 190, 263–273, https://doi.org/10.1016/S0021-9673(00)88229-1, 1980.

https://doi.org/10.5194/egusphere-2026-8
Preprint. Discussion started: 15 January 2026

Furuta, D., Sayahi, T., Li, J., Wilson, B., Presto, A. A., and Li, J.: Characterization of inexpensive metal oxide sensor performance for trace methane detection, Atmospheric Measurement Techniques, 15, 5117–5128, https://doi.org/10.5194/amt-15-5117-2022, 2022.

Gardner, J. W. and Bartlett, P. N.: A brief history of electronic noses, Sensors and Actuators B: Chemical, 18, 210–211, https://doi.org/10.1016/0925-4005(94)87085-3, 1994.

Guenther, A., Hewitt, C. N., Erickson, D., Fall, R., Geron, C., Graedel, T., Harley, P., Klinger, L., Lerdau, M., Mckay, W. A., Pierce, T., Scholes, B., Steinbrecher, R., Tallamraju, R., Taylor, J., and Zimmerman, P.: A global model of natural volatile organic compound emissions, Journal of Geophysical Research: Atmospheres, 100, 8873–8892, https://doi.org/10.1029/94JD02950, 1995.

Hagan, D. H., Isaacman-VanWertz, G., Franklin, J. P., Wallace, L. M. M., Kocar, B. D., Heald, C. L., and Kroll, J. H.: Calibration and assessment of electrochemical air quality sensors by co-location with regulatory-grade instruments, Copernicus Publications, 2018.

Hagan, D. H., Gani, S., Bhandari, S., Patel, K., Habib, G., Apte, J. S., Hildebrandt Ruiz, L., and Kroll, J. H.: Inferring Aerosol Sources from Low-Cost Air Quality Sensor Measurements: A Case Study in Delhi, India, Environ. Sci. Technol. Lett., 6, 467–472, https://doi.org/10.1021/acs.estlett.9b00393, 2019.

Han, P., Mei, H., Liu, D., Zeng, N., Tang, X., Wang, Y., and Pan, Y.: Calibrations of Low-Cost Air Pollution Monitoring Sensors for CO, NO_2, O_3, and SO_2, Sensors, 21, 256, https://doi.org/10.3390/s21010256, 2021.

Hitchman, M. L. and Saffell, J. R.: Considerations of Thermodynamics and Kinetics for the Effects of Relative Humidity on the Electrolyte in Electrochemical Toxic Gas Sensors, ACS Sens., 6, 3985–3993, https://doi.org/10.1021/acssensors.1c01339, 2021.

Hossain, S., Che, W., and Lau, A. K.-H.: Inter- and Intra-Individual Variability of Personal Health Risk of Combined Particle and Gaseous Pollutants across Selected Urban Microenvironments, International Journal of Environmental Research and Public Health, 19, https://doi.org/10.3390/ijerph19010565, 2022.

Korotcenkov, G., Blinov, I., Brinzari, V., and Stetter, J. R.: Effect of air humidity on gas response of SnO_2 thin film ozone sensors, Sensors and Actuators B: Chemical, 122, 519–526, https://doi.org/10.1016/j.snb.2006.06.025, 2007.

Kroll Group: Chamber data and species concentrations, 2025, http://krollgroup.mit.edu/publications.html, last access: 31 December 2025.

Lee, J.-Y., Dinh, T.-V., Kim, D.-J., Choi, I.-Y., Ahn, J.-W., Park, S.-Y., Jung, Y.-J., and Kim, J.-C.: Comparison of Water Pretreatment Devices for the Measurement of Polar Odorous Compounds, Applied Sciences, 9, 4045, https://doi.org/10.3390/app9194045, 2019.

Lee, S.-W., Dinh, T.-V., Park, S.-Y., Choi, I.-Y., Kim, I.-Y., Park, B.-G., Baek, D.-H., Park, J.-H., Seo, Y.-B., and Kim, J.-C.: Development of a Moisture Pretreatment Device for the Accurate Quantitation of Water-Soluble Volatile Organic Compounds in Air, Chemosensors, 11, 188, https://doi.org/10.3390/chemosensors11030188, 2023.

Lerner, B. M., Gilman, J. B., Aikin, K. C., Atlas, E. L., Goldan, P. D., Graus, M., Hendershot, R., Isaacman-VanWertz, G. A., Koss, A., Kuster, W. C., Lueb, R. A., McLaughlin, R. J., Peischl, J., Sueper, D., Ryerson, T. B., Tokarek, T. W., Warneke, C., Yuan, B., and de Gouw, J. A.: An improved, automated whole air sampler and gas chromatography mass spectrometry analysis system for volatile organic compounds in the atmosphere, Atmospheric Measurement Techniques, 10, 291–313, https://doi.org/10.5194/amt-10-291-2017, 2017.

https://doi.org/10.5194/egusphere-2026-8
Preprint. Discussion started: 15 January 2026

Lewis, A. C., Lee, J. D., Edwards, P. M., Shaw, M. D., Evans, M. J., Moller, S. J., Smith, K. R., Buckley, J. W., Ellis, M., Gillot, S. R., and White, A.: Evaluating the performance of low cost chemical sensors for air pollution research, Faraday Discuss., 189, 85–103, https://doi.org/10.1039/C5FD00201J, 2016.

Lieber, C. and Mahadevan-Jansen, A.: Automated Method for Subtraction of Fluorescence from Biological Raman Spectra, Applied spectroscopy, 57, 1363–7, https://doi.org/10.1366/000370203322554518, 2003.

Liess, M. and Leonhardt, M.: New operation principle for ultra-stable photo-ionization detectors, Meas. Sci. Technol., 14, 427–432, https://doi.org/10.1088/0957-0233/14/4/304, 2003.

Liu, H., Wu, R., Guo, Q., Hua, Z., and Wu, Y.: Electronic Nose Based on Temperature Modulation of MOS Sensors for Recognition of Excessive Methanol in Liquors, ACS Omega, 6, 30598–30606, https://doi.org/10.1021/acsomega.1c04350, 2021.

Llobet, E., Vilanova, X., Brezmes, J., Sueiras, J. E., Alcubilla, R., and Correig, X.: Steady-State and Transient Behavior of Thick-Film Tin Oxide Sensors in the Presence of Gas Mixtures, J. Electrochem. Soc., 145, 1772, https://doi.org/10.1149/1.1838556, 1998.

Lovelock, J. E.: A Photoionization Detector for Gases and Vapours, Nature, 188, 401–401, https://doi.org/10.1038/188401a0, 1960.

Luo, S., Hao, Q., Xu, Z., Zhang, G., Liang, Z., Gou, Y., Wang, X., Chen, F., He, Y., and Jiang, C.: Composition Characteristics of VOCs in the Atmosphere of the Beibei Urban District of Chongqing: Insights from Long-Term Monitoring, Atmosphere, 14, 1452, https://doi.org/10.3390/atmos14091452, 2023.

Mao, F., Khamis, K., Krause, S., Clark, J., and Hannah, D. M.: Low-Cost Environmental Sensor Networks: Recent Advances and Future Directions, Front. Earth Sci., 7, https://doi.org/10.3389/feart.2019.00221, 2019.

Mead, M. I., Popoola, O. A. M., Stewart, G. B., Landshoff, P., Calleja, M., Hayes, M., Baldovi, J. J., McLeod, M. W., Hodgson, T. F., Dicks, J., Lewis, A., Cohen, J., Baron, R., Saffell, J. R., and Jones, R. L.: The use of electrochemical sensors for monitoring urban air quality in low-cost, high-density networks, Atmospheric Environment, 70, 186–203, https://doi.org/10.1016/j.atmosenv.2012.11.060, 2013.

Murray, C. J. L., Aravkin, A. Y., Zheng, P., Abbafati, C., Abbas, K. M., Abbasi-Kangevari, M., Abd-Allah, F., Abdelalim, A., Abdollahi, M., Abdollahpour, I., Abegaz, K. H., Abolhassani, H., Aboyans, V., Abreu, L. G., Abrigo, M. R. M., Abualhasan, A., Abu-Raddad, L. J., Abushouk, A. I., Adabi, M., Adekanmbi, V., Adeoye, A. M., Adetokunboh, O. O., Adham, D., Advani, S. M., Agarwal, G., Aghamir, S. M. K., Agrawal, A., Ahmad, T., Ahmadi, K., Ahmadi, M., Ahmadieh, H., Ahmed, M. B., Akalu, T. Y., Akinyemi, R. O., Akinyemiju, T., Akombi, B., Akunna, C. J., Alahdab, F., Al-Aly, Z., Alam, K., Alam, S., Alam, T., Alanezi, F. M., Alanzi, T. M., Alemu, B. wassihun, Alhabib, K. F., Ali, M., Ali, S., Alicandro, G., Alinia, C., Alipour, V., Alizade, H., Aljunid, S. M., Alla, F., Allebeck, P., Almasi-Hashiani, A., Al-Mekhlafi, H. M., Alonso, J., Altirkawi, K. A., Amini-Rarani, M., Amiri, F., Amugsi, D. A., Ancuceanu, R., Anderlini, D., Anderson, J. A., Andrei, C. L., Andrei, T., Angus, C., Anjomshoa, M., Ansari, F., Ansari-Moghaddam, A., Antonazzo, I. C., Antonio, C. A. T., Antony, C. M., Antriyandarti, E., Anvari, D., Anwer, R., Appiah, S. C. Y., Arabloo, J., Arab-Zozani, M., Ariani, F., Armoon, B., Ärnlöv, J., Arzani, A., Asadi-Aliabadi, M., Asadi-Pooya, A. A., Ashbaugh, C., Assmus, M., Atafar, Z., Atnafu, D. D., Atout, M. M. W., Ausloos, F., Ausloos, M., Quintanilla, B. P. A., Ayano, G., Ayanore, M. A., Azari, S., Azarian, G., Azene, Z. N., et al.: Global burden of 87 risk factors in 204 countries and territories, 1990–2019: a systematic analysis for the Global Burden of Disease Study 2019, The Lancet, 396, 1223–1249, https://doi.org/10.1016/S0140-6736(20)30752-2, 2020.

https://doi.org/10.5194/egusphere-2026-8
Preprint. Discussion started: 15 January 2026

Pellizzari, E. D., Bunch, J. E., Carpenter, B. H., and Sawicki, E.: Collection and analysis of trace organic vapor pollutants in ambient atmospheres. Technique for evaluating concentration of vapors by sorbent media, Environ. Sci. Technol., 9, 552–555, https://doi.org/10.1021/es60104a008, 1975.

Pinder, R. W., Klopp, J. M., Kleiman, G., Hagler, G. S. W., Awe, Y., and Terry, S.: Opportunities and Challenges for Filling the Air Quality Data Gap in Low- and Middle-Income Countries, Atmospheric environment (Oxford, England : 1994), 215, https://doi.org/10.1016/j.atmosenv.2019.06.032, 2019.

Scott, A.: The effects of high humidity on standard PID sensor can result in errors, 2020, https://ionscience.com/in/news/effects-of-high-humidity-on-photoionisation-detectors-pids/, last access: 31 December 2025..

Snyder, E. G., Watkins, T. H., Solomon, P. A., Thoma, E. D., Williams, R. W., Hagler, G. S. W., Shelow, D., Hindin, D. A., Kilaru, V. J., and Preuss, P. W.: The Changing Paradigm of Air Pollution Monitoring, Environ. Sci. Technol., 47, 11369–11377, https://doi.org/10.1021/es4022602, 2013.

Spinelle, L., Gerboles, M., Kok, G., Persijn, S., and Sauerwald, T.: Review of Portable and Low-Cost Sensors for the Ambient Air Monitoring of Benzene and Other Volatile Organic Compounds, Sensors (Basel), 17, https://doi.org/10.3390/s17071520, 2017.

Taguem, E. M., Mennicken, L., and Romain, A.-C.: Quantile regression with a metal oxide sensors array for methane prediction over a municipal solid waste treatment plant, Sensors and Actuators B: Chemical, 334, 129590, https://doi.org/10.1016/j.snb.2021.129590, 2021.

Wang, C., Yin, L., Zhang, L., Xiang, D., and Gao, R.: Metal Oxide Gas Sensors: Sensitivity and Influencing Factors, Sensors (Basel), 10, 2088–2106, https://doi.org/10.3390/s100302088, 2010.

Wei, P., Ning, Z., Ye, S., Sun, L., Yang, F., Wong, K. C., Westerdahl, D., and Louie, P. K. K.: Impact Analysis of Temperature and Humidity Conditions on Electrochemical Sensor Response in Ambient Air Quality Monitoring, Sensors, 18, 59, https://doi.org/10.3390/s18020059, 2018.

Woolfenden, E.: Monitoring VOCs in Air Using Sorbent Tubes Followed by Thermal Desorption-Capillary GC Analysis: Summary of Data and Practical Guidelines, Journal of the Air & Waste Management Association, 47, 20–36, https://doi.org/10.1080/10473289.1997.10464411, 1997.

Xie, S., Meeker, J. R., Perez, L., Eriksen, W., Localio, A., Park, H., Jen, A., Goldstein, M., Temeng, A. F., Morales, S. M., Christie, C., Greenblatt, R. E., Barg, F. K., Apter, A. J., and Himes, B. E.: Feasibility and acceptability of monitoring personal air pollution exposure with sensors for asthma self-management, Asthma Research and Practice, 7, 13, https://doi.org/10.1186/s40733-021-00079-9, 2021.

Yang, Y., Liu, B., Hua, J., Yang, T., Dai, Q., Wu, J., Feng, Y., and Hopke, P. K.: Global review of source apportionment of volatile organic compounds based on highly time-resolved data from 2015 to 2021, Environment International, 165, 107330, https://doi.org/10.1016/j.envint.2022.107330, 2022.

You, B., Zhou, W., Li, J., Li, Z., and Sun, Y.: A review of indoor Gaseous organic compounds and human chemical Exposure: Insights from Real-time measurements, Environment International, 170, 107611, https://doi.org/10.1016/j.envint.2022.107611, 2022.

Zamora, M. L., Buehler, C., Datta, A., Gentner, D. R., and Koehler, K.: Identifying optimal co-location calibration periods for low-cost sensors, Atmos Meas Tech, 16, 169–179, https://doi.org/10.5194/amt-16-169-2023, 2023.

https://doi.org/10.5194/egusphere-2026-8
Preprint. Discussion started: 15 January 2026

Zhao, L., Wang, J., and Li, X.: Identification of Formaldehyde under Different Interfering Gas Conditions with Nanostructured Semiconductor Gas Sensors, Nanomaterials and Nanotechnology, 5, 38, https://doi.org/10.5772/62115, 2015.

635 Zusman, M., Schumacher, C. S., Gassett, A. J., Spalt, E. W., Austin, E., Larson, T. V., Carvlin, G., Seto, E., Kaufman, J. D., and Sheppard, L.: Calibration of low-cost particulate matter sensors: model development for a multi-city epidemiological study, Environ Int, 134, 105329, https://doi.org/10.1016/j.envint.2019.105329, 2020.